HHS Public Access

Author manuscript

IFAC Pap OnLine. Author manuscript; available in PMC 2024 February 26.

Published in final edited form as:

IFAC Pap OnLine. 2022 ; 55(23): 35–40. doi:10.1016/j.ifacol.2023.01.011.

Optimal Temperature Protocols for Liver Machine Perfusion Using a Monte Carlo Method

Angelo Lucia[*], **Korkut Uygun**[**]

[*]University of Rhode Island, Kingston, RI 02881-2019 USA

[**]Massachusetts General Hospital, Boston, MA 02114 USA

Abstract

Monte Carlo simulation with a novel acceptance procedure is used to find optimal temperature profiles for liver machine perfusion. Numerical results for MC simulation are compared to a greedy approach and to current practice in machine perfusion research. Results show that the proposed Monte Carlo simulation approach finds optimal temperature profiles that agree with current clinical research practice.

Keywords

liver metabolism; machine perfusion; Nash Equilibrium modeling; Monte Carlo simulation; optimal temperature protocols

1. INTRODUCTION

Static Cold Storage (SCS), i.e., flushing the organ with a solution such as University of Wisconsin (UW) solution and then placing the organ on ice, is the current gold standard for organ preservation. Unfortunately, SCS is time limited because the organ is in a hypoxic state. This depletes energy carriers like ATP and can cause a buildup of lactic acid over time that can lead to cell death if continued for too long. In addition, the number of wait-listed transplantation patients exceeds the number of available organs. Thus, many patients die before receiving a donor organ. This is, in part, because many ‘marginal’ organs are discarded because they do not meet organ viability criteria. As a result, machine perfusion (MP) is gaining acceptance as a tool for increasing the number of viable organs for transplantation. Figure 1 shows a schematic of a liver perfusion machine, in which the liver is supplied with nutrients (e.g., Williams Medium E solution) containing dissolved oxygen, often referred to a *perfusate*.

Machine perfusion is classified by the temperature protocol used; however, the two most common protocols are Subnormothermic Machine Perfusion (SNMP) and Normothermic Machine Perfusion (NMP), which use fixed temperatures of 21-34 °C and 35-37 °C respectively. Many experimental studies have shown that when marginally ischemic livers

Tel: 402-874-2814, alucia@uri.edu.

are subjected to machine perfusion there is an increase in biomarkers such as ATP content, energy charge, and bile production and concomitant clearance of lactic acid.

In a recent paper, Lucia et al. (2022) have successfully used a liver metabolism model and a Nash Equilibrium approach to simulate both SCS and warm ischemia. Numerical simulation results were compared with experimental data and demonstrate that the NE approach provides 'good' matches to experimental data.

In this paper, we use the liver metabolism model developed by Lucia et al. (2022) to simulate liver machine perfusion and couple this with Monte Carlo simulation to determine optimal temperature protocols.

2. A BRIEF LITERATURE SURVEY

Mathematical modeling of metabolism using a systems approach has a long history, dating back to Michaelis and Menton (1913). More recent pseudo-steady-state numerical modeling and simulation approaches include Flux Balance Analysis (FBA) introduced by Varma and Palsson (1994), the Mixed Integer Linear Programming (MILP) method of Lee et al. (2000), the dynamic FBA (or dFBA) method of Mahadevan et al. (2002). Unsteady-state modeling and simulation methods (e.g., Zielinski and Palsson, 2012), on the other hand, use chemical reaction kinetics to model metabolism but require many kinetic parameters, which grow exponentially with model size to regressed to data to be useful. There are also Metabolic Flux Analysis (MFA) approaches that combine the use of experimental data and systems engineering. See, for example, Yang et al. (2002), Lee et al. (2003), Uygun et al. (2007), Henry et al. (2007), Sharma et al. (2011), Orman et al. (2011a, b), and others. More recently, Lucia and coworkers have proposed a Nash Equilibrium approach to metabolic network modeling and have successfully applied the NE approach to acetyl CoA synthesis in *E Coli* (2016), the methionine salvage pathway (2018), and liver metabolism (2022).

3. METABOLIC NETWORK MODELING

3.1 Nash equilibrium modeling

The NE approach to modeling metabolic networks treats enzymes as players in a multi-player game in which each enzyme minimizes the Gibbs free energy of the reaction it catalyzes. The resulting formulation gives rise to N distinct nonlinear programming (NLP) problems in which the unknown variables are the fluxes of metabolites, cofactors, and enzymes, where N is the number of chemical reactions. Temperature effects are accounted for by using the Gibbs-Helmholtz equation and the only model parameters needed are standard state Gibbs free energy and enthalpies of formation. See Lucia et al. (2018) for a tutorial on the Nash Equilibrium approach that includes basic model formulation, linear dependence of charge balance constraints, enzymatic reactions, up/down regulation of enzymes, and feedback and allosteric inhibition.

3.2 A model of liver metabolism

The model of liver metabolism used in this paper is given in Lucia et al. (2022) and consists of three cellular compartment – the cytosol, inner membrane, and mitochondria,

27 metabolic pathways, 64 chemical reactions involving mostly charged species, 309 metabolites and cofactors, 205 mass (charge) balances, and 81 model parameters (i.e., Gibbs free energies and enthalpies of formation). Figure 2 in Lucia et al. (2022) is a superstructure representation of liver metabolism that includes inter-pathway transport.

4. LIVER MACHINE PERFUSION NUMERICS

The numerical simulation of liver machine perfusion consists of two parts – (1) SCS simulation followed by (2) the simulation of MP using a given temperature protocol. Thus, the fluxes at the end of a SCS simulation are taken as the starting point (or initial conditions) for all MP simulations. Finally, all computations were done on a Dell Vostro laptop with an Intel I7 core processor using the Lahey-Fijitsu LF95 compiler.

4.1 Base case simulations: SNMP and NMP

The base cases chosen for comparison in this study were SNMP and NMP, which both use a constant temperature protocol of 21 and 37 °C respectively at each NE iteration. Liver viability was measured using a weighted multi-objective criterion (or reward, R) that included (1) glucose consumption, (2) net ATP synthesis, (3) net mevalonate synthesis as a measure of bile production, and (4) energy charge having the form

$$R = w_1|G| + w_2 ATP + w_3 Mev + w_4 EC \tag{1}$$

where G denotes glucose consumption, ATP is the net ATP synthesis, Mev denotes mevalonate production, EC is energy charge, and w_1 through w_4 are the weights.

Following Southard et al. (1991), SCS simulations consisted of flushing the liver with the 50 ml of UW solution as shown in Table 1.

During SCS the liver receives no nutrients and is in a hypoxic state, ATP is depleted, and there is a buildup of lactate. In SNMP and NMP, cells synthesize ATP and bile (Mev), increase energy charge, and clear lactate. Tables 2 and 3 show results for SCS.

followed by *4 hours of MP* with $w_1 = w_2 = w_3 = w_4 = 1$ since all metrics are important for liver viability.

The key nutrients in the Williams Medium E solution used in the MP simulations are shown in Table 3 and consist of glucose, amino acids, and bicarbonate. The amount of oxygen dissolved in the Williams Medium E solution was determined from the solubility of O_2 at the MP temperature.

Note that the overall performance of NMP is slightly worse than SNMP as measured by the reward, largely due to much lower ATP generation. Both machine perfusion protocols increase the energy charge, consume glucose, produce mevalonate, and satisfy pH and lactate concentration constraints.

4.2 Optimization

Optimal temperature profiles are important in machine perfusion because they maximize organ viability and avoid thermal issues, which potentially improve the chances of successful transplant. The optimization problem to be solved is as follows:

$$\max_{T(t)} R \tag{2}$$

$$\text{such that} \quad pH > 7.3 \tag{3}$$

$$[lactate] < 2.3 \text{ mM} \tag{4}$$

where $T(t)$ is the *discrete* temperature protocol (or policy in machine learning terminology), $\{T_1, T_2, \ldots, T_N\}$, that can be adjusted every 30 minutes; thus, the time horizon is 4 hours as in the SNMP and NMP simulations.

4.2.1 Greedy Optimization—One intuitive way to try and improve the reward (or value of the multi-objective function) is to apply a *greedy approach*. Greedy methods chose the action that results in the highest reward at each discrete time step but do not consider future rewards. Although greedy optimization tends to be faster than many other methods and provide improvement, they often fail to find the best solution.

In this work, greedy optimizations were initialized using a SCS solution for the metabolite and cofactor fluxes and the SNMP temperature protocol. Greedy exploration was conducted using temperature changes (i.e., actions) of + 2 °C. For each choice of temperature at each 30-minute interval, a complete simulation of the Nash Equilibrium model of the liver starting from a SCS simulation followed by a MP simulation and evaluation of glucose consumed, ATP and mevalonate generated, and energy charge as well as the viability constraints (3) and (4) was required.

4.2.2 Monte Carlo Optimization—A much better way of determining the optimal temperature profile is to run complete *episodes* of SCS plus MP and use a simple but effective Monte Carlo sampling procedure to exploit the fact that any optimal discrete temperature protocol should satisfy

$$T_1 \leq T_2 \leq \cdots \leq T_N \tag{5}$$

Note that (5) allows for SNMP and NMP. Equation (5) also helps to define an acceptance rule. That is, a new temperature policy is accepted *if and only* if the following two conditions are satisfied:

$$R\left[T\left(t^{k+1}\right)\right] > R_{max}\left[T\left(t^{k}\right)\right] \tag{6}$$

$$T_1^{k+1} \leq T_2^{k+1} \leq \cdots \leq T_N^{k+1} \tag{7}$$

where $R_{max}\left[T\left(t^{k}\right)\right]$ is the best value of the reward and $T\left(t^{k}\right)$ is a candidate for the best temperature policy at the end of step k. While (6) leads to a conservative (or lower) acceptance ratio because it does not accept a policy if the reward decreases, it provides robustness to the Monte Carlo optimization approach.

The Monte Carlo optimization calculations were initialized in the same way that the greedy optimizations were initialized (i.e., using SCS fluxes of metabolites and cofactors and an SNMP temperature policy). Table 5 shows results for the greedy approach and Monte Carlo optimization with 250 steps while Table 6 gives results different numbers of Monte Carlo cycles ranging from 100 to 250.

Tables 4 and 5 show that MP with greedy optimization provides improvement over SNMP and NMP but does significantly worse when compared to Monte Carlo optimization. That is, greedy produces more bile (mevalonate) per liver cell than either SNMP and NMP and does this with very little computational overhead (12.20 CPU sec.). However, greedy optimization results in slightly less ATP generated/per liver cell than SNMP but considerably more ATP/per liver cell than NMP respectively.

Table 5 also shows that Monte Carlo optimization yields the best results but at a higher computational cost because the acceptance ratio for Monte Carlo optimization is significantly lower than that of greedy optimization. That is, MP with Monte Carlo optimization results in Tables 4 and 5 show a %, % and % improvement in ATP generation/per liver cell when compared o SNMP, NMP and greedy respectively.

The results in Table 6 show that the greatest improvement in machine perfusion performance occurs from 100 to 150 Monte Carlo cycles. After that, there are only improvements in net ATP produced and energy charge occur at the expense of glucose consumption. From 250 cycles on there is no further improvement in performance.

Table 7 gives the temperature policies as a function of Monte Carlo cycles. Note that there is a gradual difference in the temperature policy for results corresponding to 100, 150, 200, and 250 Monte Carlo cycles and concomitant gradual improvements in machine perfusion performance in using additional Monte Carlo cycles. See Table 6. Moreover, the temperature

changes at each 30-minute interval following the first hour are irregular with the largest temperature change of ~9.3 °C taking place at hour 2.

In contrast, the temperature policy for greedy optimization, $T(t) = \{T_1, T_2, \ldots, T_8\}$, was {*21, 27, 29, 29, 29, 33, 37, 37* °C} but showed a larger jump in temperature at hours 2 and 3 of four °C. Note that the qualitative results for determining optimal temperature protocols for greedy and Monte Carlo optimization are quite different. The greedy approach reaches a suboptimal solution with a reward of $R = 3.1748$ with values of ATP produced and energy charge of 1.2826 and 0.5882 respectively in 12.20 CPU sec. While much faster than Monte Carlo optimization, the greedy approach does not find the best overall MP performance.

4.2.3 Other Considerations—Since the number of Monte Carlo cycles used to determine the results in Tables 6 and 7 was small, we repeated the optimizations using 10,000 Monte Carlo cycles to ensure that the computations were not trapped in a local minimum. The results shown in Tables 6 and 7 for 250 cycles remained unchanged when 10,000 cycles were used.

Given that the Monte Carlo optimizations indicate that temperature profiles that adjust the perfusion temperature upwards periodically result in improvements in net ATP production and reward, we tried using a monotonically increasing, equally spaced temperature protocol $T(t) = \{23, 25, 27, 29, 31, 33, 35, 37$ °C}. The performance of this policy fell between SNMP and NMP with a reward, $R = 3.0647$, ATP production of 1.2834 pmol/cell, bile production of 0.2878 pmol/cell, glucose consumption of 0.9179 pmol/cell, and an energy charge of 0.5755. The corresponding lactate concentration was 1.906 mM and the pH was 7.5678.

6. CONCLUSIONS

To our knowledge, this work represents the first systematic application of optimization for the determination of temperature protocols for liver machine perfusion. A novel multi-objective function with constraints was proposed as an optimization model for liver viability prior to transplantation. Both greedy and Monte Carlo optimization were conducted and resulted in improvements in the ATP generation and energy charge of liver cells during machine perfusion. The specific example studied in this work was liver machine perfusion for 4 hours. Figure 2 shows the key results for this study for SNMP, NMP, as well as MP using greedy optimization and Monte Carlo optimization.

Results for the machine perfusion temperature policies determined by greedy and Monte Carlo showed a somewhat unexpected *unequal* temperature adjustments upward every 30 minutes after the first hour, eventually reaching body temperature after 3 and one-half hours. Monte Carlo optimization resulted in significant improvements in ATP production/glucose consumed accompanied by smaller improvements in bile production and energy charge. The larger increases in ATP production suggest the use of ATP synthesis or ATP content as a biomarker for liver graft viability prior to transplantation and reaffirms findings and recommendations reported in Berendsen et al. (2012), Bruinsma et al. (2013), and others. The Monte Carlo optimization findings also agree quite well with recent clinical *ex situ*

gradual rewarming studies in kidney machine perfusion. See, for example, Gallinat et al. (2018) and Mahboub et al. (2020).

However, much work remains to be done. Some interesting extensions of this work include studying the impact of

1. Initializing MP using different SCS simulations and initial temperature policies such as hypothermic machine perfusion (HMP) or mid-thermic machine perfusion (MMP). HMP and MMP operate at lower temperatures – 0 – 12 °C and 13 – 20 °C respectively. These lower MP temperature conserves ATP depletion and, in principle, result in lower recovery demands for machine perfusion. Nonetheless, it would be interesting to see how these lower protocols effect the performance of the greedy and Monte Carlo optimizations.
2. Optimizing the perfusate (i.e., nutrients) composition using Monte Carlo optimization. This is an important problem that has not been systematically studied before. Effort in this regard could also include studying the impact of the addition of other constituents that are not present in standard preservation solutions like Williams Medium E and Histidine-Tryptophan-Ketoglutarate (HTK).
3. Different metrics for the multi-objective function to measure MP performance. The multi-objective function used in this work is an outgrowth of the criteria described in Laing et al. (2017), which are used to assess liver viability and transplantability. However, there may be other metrics that potentially prove more valuable in this regard.

These first three extensions represent, in our mind, ‘low hanging fruit’ and have the potential to significantly improve the performance and practice of machine perfusion. Other extension that are more numerical in nature include developing

4) Better Monte Carlo acceptance rules to improve computational efficiency. As noted, the Monte Carlo acceptance rules proposed in this work, (6) and (7), are very conservative and generally yield acceptance ratios of 0.43 – 0.51, which is certainly reasonable. While these acceptance rules are within the range of ‘good’ acceptance ratios for Monte Carlo methods, it may be possible to find better acceptance rules – especially when nutrient optimizations are considered in conjunction with finding optimal temperature policies.

5) Development of a reinforcement learning framework for paring donor livers with recipients. Every donor liver is different as is each recipient. Both greedy and Monte Carlo optimization can be used within a reinforcement learning framework to determine the most suitable paring of donor livers and recipients.

ACKNOWLEDGEMENT

This material is partially based upon work supported by the National Science Foundation under Grant No. EEC 1941543. Support from the US National Institutes of Health (grants R01DK096075 and R01DK114506) and the Shriners Hospitals for Children is gratefully acknowledged.

REFERENCES

Berendsen TA, Bruinsma BG, Lee J, D'Andrea V, Liu Q, Izamis M-L, Uygun K Yarmush ML (2012). A simplified subnormothermic machine perfusion system restores ischemically damaged liver grafts in rat model of orthotopic liver transplantation. Transplantation Research 1, 6. [PubMed: 23369351]

Bruinsma BG, Berendsen TA, Izamis M-L, Yarmush ML, Uygun K (2013). Determination and extension of the limits of static cold storage using subnormothermic machine perfusion. Int. J. Artif. Organs, 36(11), 775–780. [PubMed: 24338652]

Gallinat A, Lu J, von Horn C et al. Transplantation of cold stored porcine kidneys after controlled oxygenated rewarming. (2018). Artif. Organs 42, 647–654. [PubMed: 29607529]

Henry CS, Broadbelt LJ & Hatzimanikatis V (2007). Thermodynamics-based metabolic flux analysis. Biophys J 92, 1792–1805. [PubMed: 17172310]

Laing RW, Mergental H, Yap C et al. (2017). Viability testing and transplantation of marginal livers (VITTAL) using normothermic machine perfusion: study protocol for an open-label, non-randomised, prospective, single-arm trial. BMJ Open 7, e017733.

Lee K Berthiaume F Stephanopoulos GN and Yarmush ML (2003). Profiling of dynamic changes in hypermetabolic livers. Biotechnol Bioeng 83, 400–415. [PubMed: 12800135]

Lee S, Phalakornkule C, Domach MM, Grossmann IE (2000). Recursive MILP model for finding all the alternate optima in LP models for metabolic networks. Comput Chem Eng 24, 711–716.

Lucia A and DiMaggio P (2016). A Nash equilibrium approach to metabolic network analysis. In Lectures in Computer Science 10122, 45–58.

Lucia A, Thomas E & DiMaggio P (2018). On the explicit use of enzyme-substrate reactions in metabolic pathway analysis. Nicosia G et al. (eds). Lecture Notes in Computer Science 10710, 88–99.

Lucia A and DiMaggio P (2019). A multi-scale computational approach to understanding cancer. Consoli S, Recupero DR, Petkovic M (eds). Data Science for Healthcare: Methodologies and Algorithms. 327–345. Springer Nature, Switzerland AG.

Lucia A, Ferrarese E and Uygun K (2022). Modeling energy depletion in rat livers using Nash equilibrium metabolic pathway analysis. Sci. Rep 12:3496. [PubMed: 35241684]

Mahadevan R Edwards JS and Doyle FJ 3rd. (2002). Dynamic flux balance analysis of diauxic growth in Escherichia coli. Biophys. J 83, 1331–1340. [PubMed: 12202358]

Mahboub P Aburawi M, Karimian N et al. (2020). The efficacy of HBOC-201 in ex situ gradual rewarming kidney perfusion in a rat model. Artif. Organs 44, 81–90. [PubMed: 31368159]

Michaelis L and Menten ML (1913). Die Kinetik der Invertinwirkung. Biochem Z 49, 333–369.

Orman MA, Berthiaume F Androulakis IP and Ierapetritou MG (2011a). Pathway analysis of liver metabolism under stressed condition. J. Theor. Biol 272, 131–140. [PubMed: 21163266]

Orman MA, Ierapetritou MG, Androulakis IP and Berthiaume F (2011b). Metabolic response of perfused livers to various oxygenation conditions. Biotechnol. Bioeng 108, 2947–2957. [PubMed: 21755498]

Sharma NS, Deepak N and Yarmush ML (2011). Metabolic profiling based quantitative evaluation of hepatocellular metabolism in presence of adipocyte derived extracellular matrix. PLOS One 6(5), e20137. [PubMed: 21603575]

Southard JH, van Gulik TM, Ametani MS, Vreugdenhil PK, Lindell SL, Pienaar BL, Belzer FO (1990). Important components of the UW solution. Transplantation 49(2), 251–257. [PubMed: 1689516]

Uygun K, Matthew HW & Huang Y (2007). Investigation of metabolic objectives in cultured hepatocytes. Biotechnol. Bioeng 97, 622–637. [PubMed: 17058287]

Varma A and Palsson BØ (1994). Metabolic flux balancing: Basic concepts, scientific and practical use. Bio/Technology 12, 994–998.

Yang C, Hua Q, and Shimizu K (2002). Integration of the information from gene expression and metabolic fluxes for the analysis of the regulatory mechanisms in Synechocystis. Appl. Microbiol. Biotechno 58, 813–22.

Zielinski DC, Palsson BØ (2012). Kinetic modeling of metabolic networks. Wittmann C and Lee S (eds.) Systems Metabolic Engineering. Springer, Dordrecht (2012).

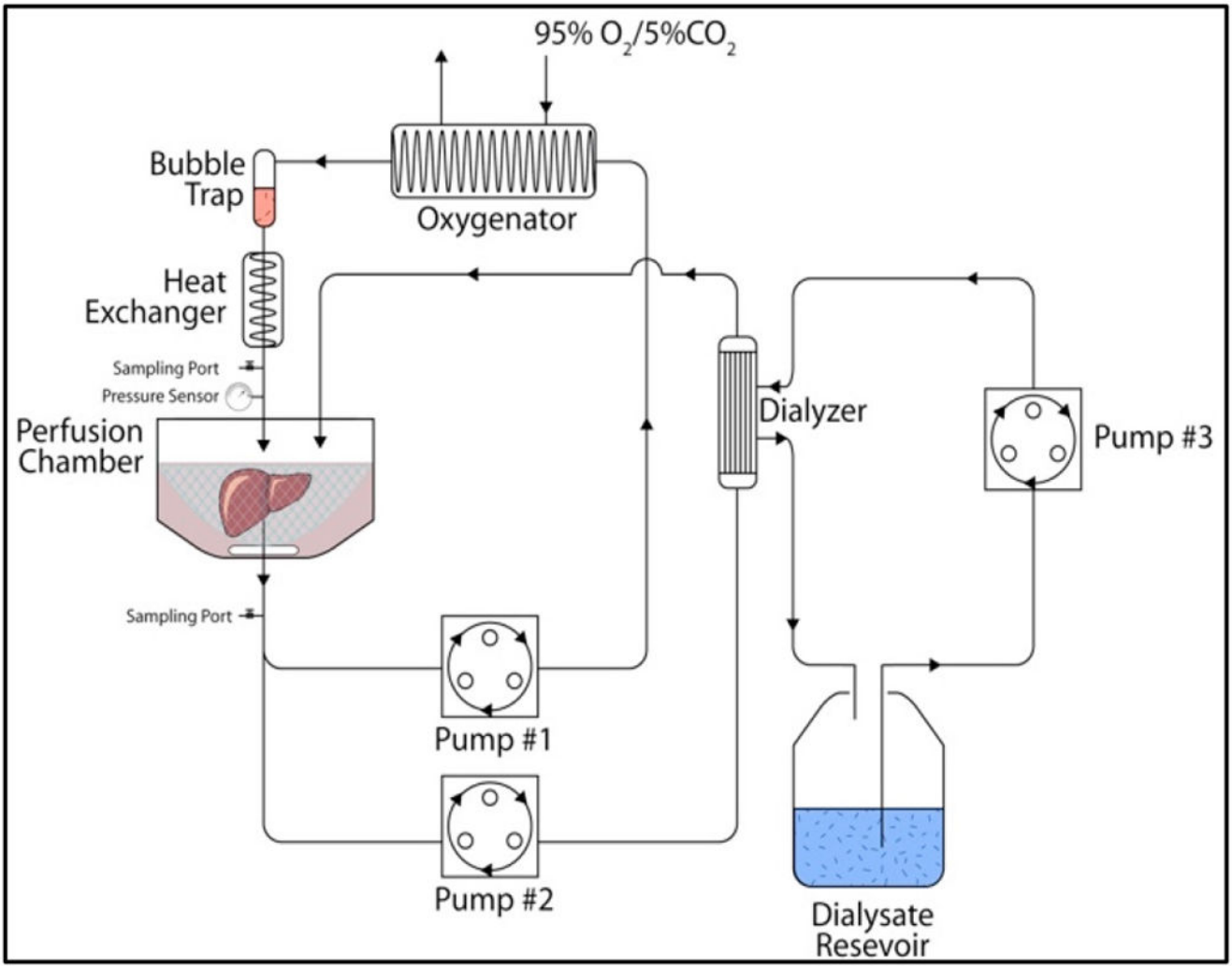

Figure 1.
Schematic of liver perfusion machine

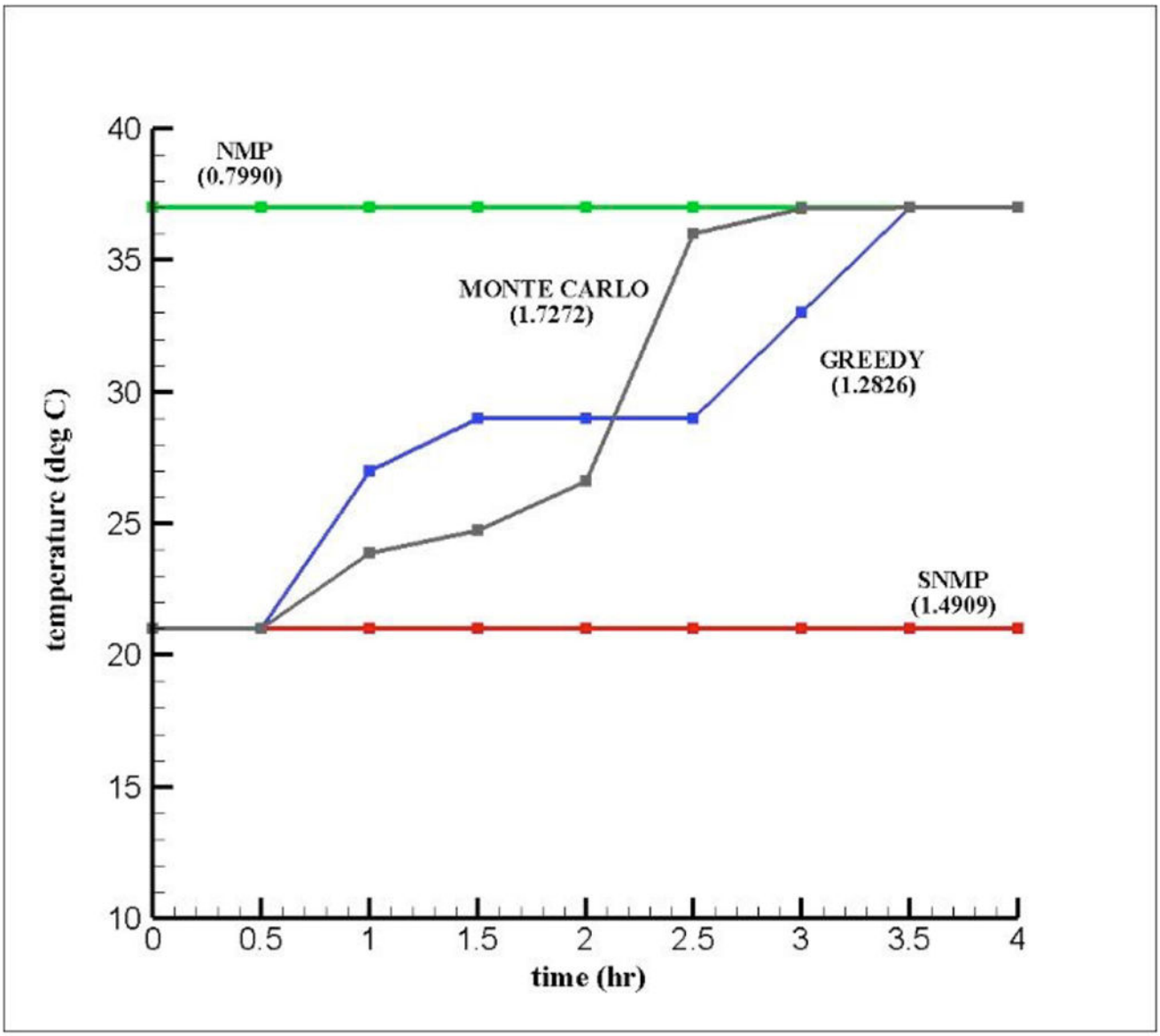

Figure 2:

Liver machine perfusion temperature policies for SNMP, NMP, GREEDY, and MONTE CARLO. Numbers in parenthesis represent amounts of ATP generated in pmol/cell.

Table 1:

UW Solution

Compound	Amount (pmol)
Glutathione	0.6
Adenosine	0.3
Water	5.54

Table 2:

Simulation Results from Static Cold Storage

T (°C)	net ATP (pmol/cell)	pH	Lactate (mM)	Energy Charge
4	−2.586	8.93	4.11	0.4395

Table 3.

Williams Medium E Components

Key Nutrients	Composition (g/L)
Glucose	2
Glutamine	0.292
Glutathione	0.00005
L-serine	0.01
Glycine	0.05
L-alanine	0.09
L-arginine	0.05
L-aspartate	0.03
L-cysteine	0.04
bicarbonate	as needed

Table 4:

Simulation Results for SNMP and NMP

	SNMP	NMP
T (°C)	21	37
$\|G\|$ (pmol/cell)	0.6185	1.122
ATP (pmol/cell)	1.4909	0.7990
Mev (pmol/cell)	0.2269	0.2898
pH	7.59	7.54
[*lactate*] (mM)	1.9354	1.9031
EC	0.5941	0.5597
R	2.9304	2.7713

Table 5:

Greedy and Monte Carlo Optimization Results

	Greedy	Monte Carlo
$\|G\|$ (pmol/cell)	1.0046	0.9308
ATP (pmol/cell)	1.2826	1.7246
Mev (pmol/cell)	0.2993	0.2936
pH	7.5526	7.5654
[*lactate*] (mM)	1.9043	1.9080
EC	0.5882	0.6024
R	3.1748	3.5514
acceptance ratio	0.6734	0.4320
Time (sec.)	12.20	87.12

Table 6:

Effect of Monte Carlo Cycles on Results

	Monte Carlo Steps			
Metric	100	150	200	250
$\|G\|$ (pmol/cell)	0.7568	0.8673	0.8841	0.9308
ATP (pmol/cell)	1.4328	1.3807	1.5749	1.7246
Mev (pmol/cell)	0.2774	0.2910	0.2912	0.2936
pH	7.5796	7.5756	7.5708	7.5654
[*lactate*] (mM)	1.9090	1.9065	1.9061	1.9080
EC	0.5928	0.5915	0.5986	0.6024
R	3.0598	3.1306	3.3489	3.5514
acceptance ratio	0.5100	0.5000	0.4500	0.4320
Time (sec)	25.71	54.10	58.09	87.12

Table 7:

Temperature Protocol vs. Monte Carlo Cycles

	Monte Carlo Cycles			
	100	150	200	250
T_1	21	21	21	21
T_2	21	21	21	21
T_3	21	21	24.38	23.87
T_4	21	26.62	26.62	26.62
T_5	21.53	28.38	28.38	35.91
T_6	26.11	35.59	35.59	36.07
T_7	31.89	36.66	36.99	37
T_8	37	37	37	37